Journal of Oceanography and Marine Research
ISSN: 2572-3103
Ramos e Silva et al., J Oceanogr Mar Res 2017, 5:1
DOI: 10.4172/2572-3103.1000155
Research Article
OMICS International

Variability and Transport of Inorganic Carbon Dioxide in a Tropical Estuary

Ramos e Silva CA[1-3*], Davalos PB[2], Silva MP[4], Miranda LB[5] and Calado L[6]

[1]Department of Oceanography and Limnology, Rio Grande do Norte Federal University, Brazil
[2]Postgraduate Program in Dynamics of Oceans and Earth, Fluminense Federal University, Brazil
[3]Center for Study of Water, Biomass and Oil (NAB), Fluminense Federal University, Brazil
[4]Department of Geophysics, Rio Grande do Norte Federal University, Brazil
[5]Department of Physical Oceanography, São Paulo University, São Paulo, Brazil
[6]Admiral Paulo Moreira Marine Research Institute, Arraial do Cabo, RJ-28930-000, Brazil

Abstract

Marine ecosystems are a known net source of greenhouse gases emissions. On the other hand, the geochemical fluxes, particularly from the developing countries estuarine areas, are poorly evaluated. In the present study, temporal and longitudinal water samplings were taken hourly and seasonally during full semidiurnal tidal-cycles, along the Caravelas estuary, located in northeast region of Brazil. It was analyzed the pH, total alkalinity, aragonite saturation state, calcite saturation state, dissolved inorganic carbon, aqueous CO_2 and partial pressure of CO_2 found in estuarine waters. Results showed that the total alkalinity values decreased from the estuary mouth up-river during the dry season, which reflects the low buffering capacity of river water. The estuarine total alkalinity and dissolved inorganic carbon fluxes were significantly higher in the dry season during the spring tide. The spring and neap tides were typically oversaturated with CO_2 in both the dry and rainy seasons. The highest average values were found in the dry season for both the neap and spring tides, while the CO_2 air-water flux values throughout the dry and rainy seasons, retained a positive variation range. Finally, the annual surface water flux of dissolved inorganic carbon revealed to be positive suggesting dissolved inorganic carbon exportation to coastal water.

Keywords: Carbon dioxide; Estuaries; Flux data; Air-water flux

Introduction

CO_2 sources, fluxes, mechanisms of transport, and transformation are important issues in the field of oceanography. Inorganic CO_2 may present with major spatial and temporal variability within the same estuarine system. This is due to both the complex hydrodynamics and geomorphology of this transition system [1] and the complex CO_2 chemistry in seawater [2-4]. The river area within an estuary can, for example, act as a source of CO_2 to the atmosphere, whereas a higher salinity zone, with higher primary productivity according to the availability of nutrients, can act as a sink for atmospheric CO_2 [5].

Mangrove forests which cover the shores of estuaries act as a source of organic matter once fallen leaves are decomposed by respiratory activity of bacteria, producing CO_2 [6,7]. Furthermore, the usually turbid water found in tropical estuaries provide an intense respiratory activity, thereby generating a high CO_2 partial pressure compared to air and as a consequence, such waters can act as a source of CO_2 to the atmosphere [8].

The hydrology of hypersaline and positive tropical estuarine systems is strongly influenced by rainy and dry seasons [9]. In addition, rain is responsible for runoff, leading to decreased water transparency, a decrease in pH and saturation of CO_2 [9]. Ruiz-Halpern et al. [10] also suggest that in many sub-tropical estuaries, floodplain wetlands, can deliver low pH and dissolved oxygen into the estuarine water.

In addition to metabolic shifts between net autotrophy and heterotrophy in coastal waters [11], chemical controls involved in the carbonate system can determine important changes in air-water CO_2 fluxes. CO_2 gas is dissolved in seawater, and carbonic acid (H_2CO_3) is formed from this reaction. In fact, H_2CO_3 undergoes a series of dissociation reactions that are responsible for the release of hydrogen ion (H^+). The concentration of H^+ (mol/kg) determines the acidity of the solution, which is usually expressed in the pH scale (pH=-log $[H^+]T$, total scale) [12-14]. Many biogeochemical processes and marine organisms (e.g. phytoplankton) can be affected by a decrease in pH [15-17]. The saturation state of calcium carbonate (Ω) (aragonite and calcite), for example, is also affected by pH, since the increase in concentrations of H^+ reduces the availability of the carbonate ion $CO_3^{2-} + H^+ = HCO^-_3$ (low acid concentrations) that is responsible for the formation of calcium carbonate [17-19].

Calcification affects Total Alkalinity (TA), reducing its value twice in the water column. Changes in TA are used as an indicator of the production or dissolution of calcite or the respiratory activity of organisms [20].

The aim of this study is to characterize the Caravelas estuary, BA, Brazil, from the standpoint of the transport of the components of the carbonate system and the CO_2 flux between the water and the atmosphere. A further goal is to estimate the dynamics of inorganic carbon in the dry (August) and rainy (January) seasons under the different seasonal conditions of the tide and river flow in the estuary. It is therefore essential to evaluate how TA, the surface water saturation states of calcite (Ω calc) and aragonite (Ωarag), and the balance of the transport of these chemical components towards a coastal zone are affected by different estuarine forcing.

***Corresponding author:** Ramos e Silva CA, Department of Oceanography and Limnology, Rio Grande do Norte Federal University, Natal/RN, CEP 59075-970, Brazil, Tel: +55 21 99591040; E-mail: caugusto_99@yahoo.com

Received January 09, 2017; **Accepted** February 24, 2017; **Published** March 03, 2017

Citation: Ramos e Silva CA, Davalos PB, Silva MP, Miranda LB, Calado L (2017) Variability and Transport of Inorganic Carbon Dioxide in a Tropical Estuary. J Oceanogr Mar Res 5: 155. doi: 10.4172/2572-3103.1000155

Material and Methods

Site description

The Caravelas estuary, which is located on the northeastern coast of Brazil, in Bahia state, is a tropical coastal plain environment. It is formed by the Cupido and Macacos rivers, which bathe the city of Caravelas (17°44'00S Lat., Long. 39°15'59W). This estuary is of great socioeconomic and environmental importance, because it is located near Abrolhos National Park, about 60 km from the coast, and constitutes the largest coral reef in the southern Atlantic Ocean (Figure 1). The climate is tropical humid, and is influenced by easterly winds from March to September and northern and northeasterly winds from October to February. The average annual rainfall is 1,800 mm, and is concentrated in the summer period [21].

The Caravelas estuary is influenced by freshwater discharge from two major rivers: the Caravelas in the northern section, near the town of Caravelas, which flows into the adjacent ocean through two outputs (Barra Velha and Boca do Tomba (Figure 1); and the freshwater input into the estuary, which also comes from several tributaries, such as the Cupido River.

Local tide classification

To classify the local tide during our observations, form-number N_f was calculated, as defined by Defant [22], using the amplitude values of the main diurnal and semidiurnal tide harmonic constituents in the location. These are estimated by Franco [23] as K_1=5.8 cm, O_1=8.9 cm, M_2=75.1 cm and S_2=43.7 cm, respectively. It was ascertained that the form-number for this study area was equal to N_f=0.12.

Sampling design

Hydrographic campaigns were carried out in August 2007 and January 2008, during eight tide-cycles. There were four 13-h cycles corresponding to the temporal evaluation, in the neap and spring tide conditions. The other four campaigns were carried out focusing spatial evaluation, in the same tidal conditions. These samples were taken from three spots (S_1, S_2 and S_3) along the estuary in two consecutive high and low tides per cycle (Figure 1). Two samples were collected from each spot in the mixing zone (MZ), 1 m below the water surface and 1 m above the bottom floor. There were thus 16 samplings per spot, totalizing 48 samples in four cycles.

For the temporal evaluation, 14 samples were collected during 13 h cycles at intervals of one hour from 1 m below the water surface at spot S1, producing a total of 56 samples in a two-season period (dry and wet).

All of the samples were obtained using a 5L Van Dorn bottle. Simultaneously, we obtained data on temperature, salinity and current using a current meter associated with Valeport electronic CTD sensors, model 108MkIII/308.

Measurements of the sectional area of the channel at spot S1 were taken using a Furuno LS-4100 echo sounder attached to a GARMIN GPS 12XL. It was thus possible to obtain details of the area, which is 4054 m^2, at a depth of 0.0 m (Average Low Water Springs-MLWS).

Analyses

The oxygen samples were transferred to 300 mL BOD bottles (Kimble), fixed and determined according to Winkler's method [24]. Based on salinity and temperature data, each dissolved oxygen concentration was transformed into percentage saturation. The total alkalinity was determined in the water collected in 300 mL BOD reagent bottles (Kimble) poisoned with mercuric chloride, $HgCl_2$ [25]. This was followed by a calculation with an open cell titration system according to the recommendations of Van den Berg and Rogers [26].

The pH was determined from the water collected as described above according to the methodology defined by Millero et al. [27] and Millero [12] for estuarine waters, where the "Tris" buffer was signed in the lab with an m-cresol purple indicator [25,28] through a Varian Instruments Cary 100 UV-VIS spectrophotometer using the DAO program. The batch of buffer was stored according to the method of Nemzer and Dickson [29], and all of the pH values were referred to 25°C to avoid a temperature effect of pH measurement [30]. Later, the pH values were corrected to enable environment temperature sampling.

Samples for dissolved inorganic nutrients to attain carbonate alkalinity were filtered (except from ammonia samples) through 0.45 µm cellulose acetate membranes. Analyses were carried out using a Varian Instruments Cary 100 UV-VIS spectrophotometer [24]. NH_3 samples were treated with 4.5 M H_2SO_4, purged for 2 min with N_2 (research grade) and analyses were carried out using a Varian

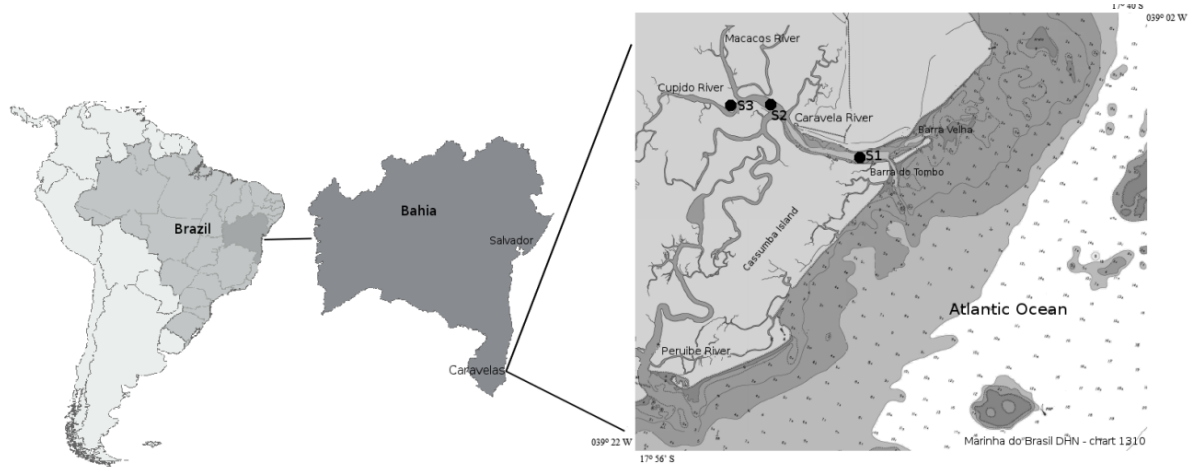

Figure 1: Study area. A: In context of Brazil and Bahia state; B: Estuarine complex of Caravelas estuary. The symbols S1, S2 and S3 indicate the sampling spots [56].

Instruments Cary 100 UV-VIS spectrophotometer, according to the methodology according to Grasshoff et al. [24].

Total concentration of calcium and boron were obtained through equations developed by Millero [31,32]. This was possible due to the proximity of estuarine water ionic strength to seawater (S=35).

All of the inorganic CO_2 systems (CO_2, CO_3^{2-}, HCO_3^-, DIC, ρCO_2, ΩCalc and ΩArag) were calculated using carbonate system dissociation K, which are defined below: $-\ln k_B^*$ - [33]; $-\ln k_{Si}^*$ - [32]; $-\ln k_1^*(H_3PO_4)$ -[34]; $-\ln k_2^*(H_2PO_4^-)$ - [34]; $-\ln k_3^*(HPO_4^{2-})$ -[34]; $-\ln k_2^*(CO_3^{2-})$ - [35].

Aqueous carbon dioxide concentrations, CO_2 partial pressures, and CO_2 water/atmosphere fluxes were calculated using a number of measurements obtained from various environmental variables (temperature, salinity, pH and TA), and from thermodynamic and stoichiometric K $(pk_1^o, pk_2^o, pk_1^* \text{ e } pk_2^*)$ as defined by Millero et al. [3]. The DAO software was also used to facilitate the calculations. The assumed atmospheric pressure of CO_2 was 380 ppm [36]. This value seems plausible, for the reference year 2005, in the study area, according to data provided by CDIAC (Carbon Dioxide Information Analysis Center).

The procedures described above were obtained with the DAO program, which is a very ordinary and simple-to-use MS Excel version.

Some stoichiometric and thermodynamic K were calculated using DAO program, making reference to the values proposed by Millero et al. [3], Wolf-Zeeb and Gladrow [14] and Pankow [37] in order to validate the program (Table 1). From data proposed by Roy et al. [35] to pH=8.08; DIC=2 mmol/kg; Salinity=35; temperature=25°C and TA=2.35 mmol/kg; calculated using DAO program ñCO_2, $CO_{2(aq)}$, HCO_3^- and CO_3^{2-}. These calculated values were compared to those reached using DAO program. Zeeb-Gladrow and Wolf [2] used the same data as Roy et al. [35]. We consider them as being satisfactory results (Table 1) [37].

Transport of properties

For the transport of properties, the equation proposed by Miranda et al. [38] was used:

$$\phi_c = \overline{\rho}\left\langle \overline{c}\,\overline{u} \right\rangle \quad (1)$$

Where $\overline{\rho}$, $\overline{c}$ and $\overline{u}$ are the average values along the water column of density, concentration and the longitudinal component of velocity, which passes through cross-section A. The symbol <> averages the average value calculated in a tide-cycle.

The direction of the u component was determined after the decomposition of the velocity vector in relation to the axis orientation of the estuary, where positive flux features export, and negative flux features import, a given property. The area of the section was determined at every sampling opportunity according to the height of the tide, extrapolating the area of the channel in relation to the angle of incidence of each margin. The density was calculated using the International Equation of the State of Sea Water.

The classical stratification-circulation diagram theoretically derived by Hansen and Rattray [39] establishes quantitative criteria to classify estuaries from their nearly-steady salinity and the longitudinal velocity component properties. This method, which is largely used for its simplicity in setting parameters for classification, as well as for the large number of estuaries included in it, calculates the relative contribution of the advective and diffusion processes to the up-estuary salt transport.

Alternatively, the main forcing mechanisms for the circulation and mixing processes and the stability characteristics of the estuary during the tidal-cycle can be analyzed by the classic Richardson estuarine Ri_e dimensionless number, defined by Fischer [40] and Bowden [41,42], as shown below:

$$Ri_e = \frac{g\frac{\Delta_{\tilde{n}H}}{\tilde{n}}Q_f}{Bu_{rms}^3} \quad (2)$$

where g, Δ_{pH}, $\overline{\rho}$, B, Q_f, and u_{rms} are: The modulus of the gravity acceleration, the difference between the density of the river and seawater, the average value of the density along the water column, the estuary width, the river discharge and the residual velocity, and the root average square of the u-velocity component that controls the intensity of tidal stirring, respectively.

Moreover, according to Fischer [40], if Ri_e is large, the estuary is stratified and the movement is dominated by fresh water discharge. Consequently, if Ri_e is small, the estuary is weakly-stratified vertically, resulting in the condition of a well-mixed estuary. Generally, the transition between these two conditions occurs when $0.08<Ri_e<0.8$.

The physical interpretation of the layer Richardson number, according to Dyer and New [43], is as follows: where $Ri_e>20$ the water column is highly stable with low vertical mixing; when $Ri_e<20$, the bottom turbulence becomes effective in causing a vertical mixing process in the water column. However, below the critical value of $Ri_e \approx 2$, the turbulent mixing makes the water column unstable. In other words, it compares the stabilizing capacity of the vertical gradient of density (salinity) with that of the destabilizing shear velocity.

All of the samples were subjected to the Shapiro-Wilks adhesion normality test and the Levenes homogeneity test, while for the comparison between populations, the non-parametric Kruskal Wallis test was used. All of the statistical tests were run by the program Statistica 7.0, StatSoft. Inc., using a significance level of $p<0.05$.

Air-sea CO_2 fluxes

The CO_2 formulation flux between oceans and the atmosphere is defined between aqueous CO_2 and saturated CO_2, as shown below:

$$F_{CO2}=k_T[CO_2 \text{ water} - CO_2 \text{ saturated}] \quad (3)$$

CO_2 and saturated CO_2 are components that characterize the "balance" of the flux equation (eq. 3), and were determined in this study using the DAO program.

Wind speed has a significant effect on the gas transfer equation. The relationship between gas exchange and wind speed can have non-linear effects on the calculation of the gas transfer velocities for particular measurements of wind speed, which will depend on the sampling design of the wind speed.

The most important parameter in the gases transfer velocity equation in terms of the function with wind speed is based on the gaseous exchange coefficient (kT in cm/h):

$$k_T = 0.31 \times u^2 \times \left[\frac{S_C}{660}\right] - 0.5 \quad (4)$$

Where u is the wind speed module at 10 m from the surface in ms^{-1}, Sc is the Schmidt number of CO_2 in seawater [44,45], and 660 is the Sc value in seawater at 20°C.

The Schmidt number is defined as the water kinematic viscosity divided by a gas diffusion coefficient, defined by a polynomial.

Source	Data Input		Data Output								
	Temp	Sal	pK_0^0	pK_1^0	pK_2^0	pK_W^0	pK_1^*	pK_2^*	pK_W^*	pK_{PS} Calc	pK_{PS} Arag
DAO	25.0	0.0	1.47	6.35	10.33	14.00					
Pankow	25.0	0.0	1.47	6.35	10.33	14.00					
Relative Error			**0%**	**0%**	**0%**	**0%**					
DAO	1.1	3.467					6.36	9.97			
Millero et al.	1.1	3.467					6.08	9.37			
Relative Error							**4.6%**	**6.4%**			
DAO	25.0	33.998					5.91	9.42			
Millero et al.	25.0	33.998					5.84	8.96			
Relative Error							**1.2%**	**5.1%**			
DAO	25.0	35.0							13.22	6.37	6.19
Zeebe and Wolf-Gladrow	25.0	35.0							13.22	6.37	6.19
Relative Error									**0%**	**0%**	**0%**

Source	Data Output		
	pCO_2 (µatm)	$CO_{2(aq)}$ (µmol/kg)	HCO_3^- (µmol/kg)
Zeebe and Wolf-Gladrow	363	10.3	1739
DAO	358	10.0	1702
Relative Error	1.37%	2.91%	2.17%

Table 1: DAO program validation data. Data input: pH=8.08; DIC=2 mmol/kg; Salinity=35; Temperature=25°C and TA=2.35 mmol/kg.

$$S_C=A-BT+CT^2-DT^3 \quad (5)$$

The constants shown above (eq. 5) are defined by Wanninkhof [46]. The kT calculation (eq. 4) takes into consideration the fact that the wind speed (u) has a fundamental quadratic dependence for the CO_2 flux calculation. Normally, the wind speed sampling for the kT calculation takes the climatological average into account at 10 m above the water surface [46]. However, such a procedure can include an error that is related to the average wind incompatibility and the CO_2 sampling "*in situ*." Moreover, the fact that the 10 m-above-water-surface wind speed reading may produce an inaccurate result due to the orographic wind-average induced by vegetation should also is taken into consideration. Accordingly, the closer to the water surface the wind speed measurements are taken, the more significant the wind effect on the Sc will be.

Consequently, in this work, the sampling design for measuring wind speed has taken this parameter to be 3 m above the water surface. In an estuary, such a procedure allows consideration of the wind speed close to the water surface without any orographic interference from local vegetation. Nevertheless, the fall in the wind speed measured at 10 m above the water surface is significantly irrelevant in comparison to the associated error caused by the orographic vegetation effect in an estuary. This corroborates the results obtained by Smith and Kemp [47] when they analyzed the iteration between wave production and wind speed in an estuary from the height where the data was taken. As a result, the authors concluded that measuring winds at 1 m above the water surface is an option when it comes to better adjusting the iteration between the water/air and minimizing the orographic errors caused by terrain morphology and trees.

Results and Discussion

The maximum tidal heights measured were 1 m and 2.95 m in the dry season in neap and spring tides conditions, respectively, and 1.48 m and 2.51 m in the rainy season, respectively, in the same tides conditions. On the other hand, the Form Number calculated for the tide in the region is equal to $N_f=(K1+O1)/(M2+S2)=0.12$. During the samplings and according to the criteria established in Miranda et al. [48] and references therein, the Caravelas estuary was classified as being a mesotidal estuary exhibing semidiurnal characteristic.

Longitudinal sample

The temperatures were practically constants in the three longitudinal spots, with the highest values found in the rainy season (28.43 ± 0.61°C). This temperature uniformity among the spots occurred due to similar depths (≈7.6 m) and the spots being in the same geographic location, which are conditions that provide the same heat capacity among the spots (Cp=dH/dT) [32,49]. The longitudinal variation in salinity values was more pronounced in the rainy seasons, showing a variation of five units (Table 2). The average salinity remained below 35 during the dry and rainy seasons, where rainfall was shown to have little influence on the salinity values during the sampling months.

In terms of the Oxygen Saturation State (OSS), the variation was evident between the seasons, with the lowest value recorded during the rainy season (spot S3), indicating a predominance of respiratory activity (70.59 ± 10.34%). Although oxygen solubility represents a salinity/temperature function [50], biological production and respiration can also affect OSS values in aquatic systems [9,51]. Farming activities (17,420 ha) and cattle breeding (63,504 animals) also influence this parameter, playing the role of an organic matter source. The difference in the OSS between the seasons in this particular estuary is not related to temperature, since both seasons presented a similar variation. Organisms consume oxygen to decompose organic matter and can therefore be responsible for lowering the dissolved oxygen saturation,

Properties	Point	Dry season		Rainy season	
		Mean and SD Per point	Mean and SD Per season	Mean and SD Per point	Mean and SD Per season
Temperature (ºC)	1	25.01 ± 0.57 (24.41-25.81)	25.04 ± 0.52 (24.41-26.01)	28.15 ± 0.48 (27.48-28.88)	28.43 ± 0.61 (27.48-29.53)
	2	25.16 ± 0.63 (24.54-26.01)		28.54 ± 0.61 (27.72-29.35)	
	3	24.95 ± 0.36 (24.53-25.45)		28.60 ± 0.70 (24.53-25.45)	
Salinity (psu)	1	33.55 ± 1.13 (34.07-37.01)	33.90 ± 2.01 (30.31-37.01)	35.24 ± 1.07 (33.78-36.40)	33.10 ± 2.33 (28.91-36.40)
	2	34.10 ± 1.68 (32.33-36.57)		33.21 ± 1.75 (31.45-35.91)	
	3	32.05 ± 1.47 (30.31-33.97)		30.87 ± 1.65 (28.91-33.26)	
pH	1	7.86 ± 0.11 (7.69-7.96)	7.75 ± 0.14 (7.49-7.96	7.93 ± 0.08 (7.82-8.03)	7.77 ± 0.18 (7.41-8.03)
	2	7.76 ± 0.14 (7.59-7.92)		7.75 ± 0.16 (7.51-7.97)	
	3	7.64 ± 0.10 (7.49-7.73)		7.60 ± 0.12 (7.41-7.73)	
OSS (%)	1	89.30 ± 7.64 (81.81-101.18)	85.62 ± 7.39 (74.62-101.18)	77.45 ± 8.49 (69.63-91.76)	70.59 ± 10.34 (55.11-91.76)
	2	86.69 ± 8.03 (79.53-99.49)		70.60 ± 11.92 (55.11-89.17)	
	3	80.89 ± 3.76 (74.62-86.30)		63.72 ± 5.42 (57.24-71.04)	

Table 2: Chemical properties during dry and rainy season.

particularly in the rainy season. This occurs because of rain, which can lead to runoffs from the drainage system that is adjacent to the estuary. The OSS in the spring tide had a positive correlation with pH and salinity (above 78%, $p<0.05$), suggesting that these results might be associated with the seawater mass along the tidal excursion. On the other hand, there was no correlation between these variables in the neap tide.

The chemical variables such as pH, ΩArag, and ΩCalc were directly related to the CO_2 inorganic system [52], and showed lower values in spot S3 during the dry and rainy seasons. The content of CO_2 correlates with pH. Dissolved CO_2 reacts with the water to form carbonic acid (H_2CO_3) which can dissociate itself up to CO_3^{2-} and H^+ decreasing the pH in the solution [53]. The lowest average values were recorded in the rainy season at spot S3, to pH=7.60 ± 0.12, to ΩCalc=3.09 ± 0.89, to ΩArag=2.04 ± 0.60 (Tables 2 and 3) and to CO_3^{2-} (112 ± 37 µmol/kg). Low concentrations of CO_3^{2-} can be explained by reactions 6 and 7, which result in a decrease in the saturation state of calcium carbonate [31].

$$H^+ + CO_3^{2-} = HCO_3^- \quad (6)$$

$$CO_2 + CO_3^{2-} + H_2O = 2HCO_3^- \quad (7)$$

Heavy rainfall ranging from 16.8 mm to 23.57 mm under the neap and spring tides, respectively (five days before the sampling, including the actual day), prior to the sampling period, might also have led to an increased rainfall-runoff from agriculture [54], resulting in the lowest pH values reported (Table 1). Furthermore, rainwater is naturally acidic because of atmospheric carbon dioxide. As rain falls into the estuary, each drop becomes saturated with CO_2 resulting also in the fall of the pH values. The correlation between these two variables (pH and CO_2) was negative (88-95%; $p<0.05$). Low pH values are responsible for the lower values of the saturation state of carbonate (Table 3) once this state is dependent on the carbonate concentration. In addition, this carbonate concentration is greatly influenced by pH.

In this study, the concentrations of calcium ions in seawater varied very little (<1.5%), averaging that the variations in the carbonate ion concentrations will rule the saturation state of calcite and aragonite [15]. This process strengthens our hypothesis that the higher production of CO_2 in spot S3 (dry season: 37.07 ± 10.15 µmol/kg and rainy season: 32.66 ± 9.81 µmol/kg) in relation to spot S1 in the dry and rainy seasons is responsible for the lower concentrations of carbonate ion in spot S3 (112 µmol/kg) (Table 3). The CO_2 aqueous pressure in spot S3 (dry season: ρCO_2=1,283 ± 346 µatm and rainy season: 1,223 ± 347 µatm) is nearly double the value found in spot S1 in both the dry and rainy seasons (Table 3). Such data reinforces the organic matter mineralization predominance in spot S3. During spring tide-cycles, the OSS and aqueous ρCO_2 had very negative correlations (dry season=-0.82%; rainy season=-0.66%; $p<0.05$).

There was a major difference in the values of the carbonate system (TA, HCO_3^-; DIC and ρCO_2) between the dry and rainy seasons among S3 and the other sampling spots during the sampling period. These values show that the estuarine water up river is under a major contribution related to organic sources originated from anthropic activities and mangrove vegetation (Table 3). The TA values in dry season (2,661 ± 98 µmol/kg) were above those found by Ramos e Silva et al. [9] for eutrophic estuaries (TA ranges from 1,600 to 2,210 µmol/kg). The average DIC values in this study varied greatly between the dry and rainy seasons (Table 3), respectively (2,356 µmol/kg and 1,891 µmol/kg), being the highest values found at S3. Low pH values and high TA concentrations can be associated with the production of HCO_3^- at S3, which is the main chemical component of TA (≈97%). In this study, given that the mixing zone (MZ) is a reducing environment, where the oxygen saturation values were below 75% in the rainy seasons at S3 (Table 2), our hypothesis of solubility of CO_2 in water producing bicarbonate ion ($CO_2 + H_2O = HCO_3^- + H^+$) is quite plausible. The studied mangrove forest acts as a source of organic carbon which favors an increase in ρCO_2 1,223 µatm (≈1.2 bar) through respiratory activity of bacteria. Furthermore, smaller concentrations of CO_3^{2-} at S3 (dry season: 127 ± 32 µmol/kg and rainy season: 112 ± 37 µmol/kg)

Properties	Point	Dry season		Rainy season	
		Mean and SD Per point	Mean and SD Per season	Mean and SD Per point	Mean and SD Per season
TA ($\mu mol\ kg^{-1}$)	1	2626 ± 61 (2541-2740)	2661 ± 98 (2450-2899)	2088 ± 243 (1517-2288)	2130 ± 222 (1517-2403)
	2	2660 ± 123 (2560-2899)		2113 ± 269 (1644-2375)	
	3	2577 ± 93 (2450-2756)		2199 ± 140 (2002-2403)	
$CO_{2\ (aqueous)}$ ($\mu mol\ kg^{-1}$)	1	20.91 ± 6.95 (13.24-31.48)	28.68 ± 10.98 (13.24-53.68)	12.16 ± 3.37 (8.44-17.00)	21.76 ± 11.90 (8.44-49.14)
	2	28.06 ± 9.75 (17.63-42.53)		21.83 ± 11.27 (12.00-40.11)	
	3	37.07 ± 10.15 (29.02-53.68)		32.66 ± 9.81 (22.74-49.14)	
CO_3^{2-}($\mu mol\ kg^{-1}$)	1	224 ± 55 (151-302)	180 ± 68 (83-302)	236 ± 60 (164-316)	171 ± 74 (60-316)
	2	188 ± 74 (114-299)		159 ± 63 (89-279)	
	3	127 ± 32 (83-162)		112 ± 37 (60-153)	
HCO^-_3($\mu mol\ kg^{-1}$)	1	2055 ± 148 (1787-2216)	2148 ± 120 (1787-2315)	1550 ± 198 (1099-1712)	1698 ± 232 (1099-2048)
	2	2185 ± 69 (2086-2303)		1698 ± 263 (1295-2048)	
	3	2203 ± 74 (2074-2315)		1869 ± 87 (1764-1997)	
DIC ($\mu mol\ kg^{-1}$)	1	2301 ± 116 (2072-2398)	2356 ± 98 (2072-2639)	1797 ± 223 (1272-1949)	1891 ± 222 (1272-2191)
	2	2401 ± 76 (2310-2539)		1879 ± 265 (1436-2191)	
	3	2367 ± 78 (2242-2509)		2014 ± 105 (1872-2176)	
PCO_2 (μatm)	1	737 ± 240 (481-1115)	1001 ± 374 (481-1851)	463 ± 126 (325-640)	821 ± 439 (325-1802)
	2	984 ± 335 (642-1491)		829 ± 421 (454-1512)	
	3	1283 ± 346 (1004-1851)		1223 ± 347 (856-1802)	
pK*2 ($mol\ kg^{-1}$)	1	9.44 ± 0.02 (9.41-9.46)	9.42 ± 0.03 (9.37-9.46)	9.39 ± 0.02 (9.36-9.42	9.36 ± 0.04 (9.29-9.42)
	2	9.42 ± 0.02 (9.39-9.45)		9.35 ± 0.03 (9.32-9.41)	
	3	9.39 ± 0.02 (9.37-9.41)		9.32 ± 0.03 (9.29-9.36)	
Ω Calc	1	5.18 ± 1.08 (3.70-6.67)	4.53 ± 1.33 (2.31-6.70)	5.53 ± 1.22 (3.90-7.15)	4.25 ± 1.51 (1.81-7.15)
	2	4.53 ± 1.48 (2.99-6.70)		3.99 ± 1.30 (2.45-6.41)	
	3	3.34 ± 0.69 (2.31-4.01)		3.09 ± 0.89 (1.81-4.15)	
Ω Arag	1	3.41 ± 0.72 (2.44-4.42)	2.86 ± 0.89 (1.51-4.44)	3.68 ± 0.82 (2.60-4.76)	2.82 ± 1.01 (1.19-4.76)
	2	2.99 ± 0.99 (1.96-4.44)		2.65 ± 0.87 (1.62-4.27)	
	3	2.19 ± 0.46 (1.51-2.64)		2.04 ± 0.60 (1.19-2.75)	

Table 3: Chemical properties during dry and rainy season.

explain the higher concentrations of HCO^-_3 at S3 (dry season: 2,203 ± 74 µmol/kg and rainy season: 1,869 ± 87 µmol/kg) which can be formed according to reaction (6). Cai and Wang [8] studied the carbon dioxide found in estuarine waters and suggested that the aerobic degradation of organic matter can have an effect on TA.

Temporal sampling

The saturation of the Mixing Zone (MZ) water related to aragonite and calcite is only a part of tropical water mass intrusions and coastal currents in the continental shelf. The concentrations of carbonate ion determine imperatively the precipitation of calcium carbonate (Section 3.1) within the MZ. The concentration of carbonate ion is the component that rules the saturation state of calcite and aragonite [15]. The salinity was nearly constant in the MZ throughout the sampling period, and did not undergo any major changes over the cycles and seasons (Table 4). The correlation of the amplitude of tides and pH

Properties	Dry season		Rainy season		Mean
	Neap	Spring	Neap	Spring	
Salinity (psu)	34.32 ± 0.50 (33.98-35.60)	35.02 ± 0.97 (33.23-35.82)	34.80 ± 0.60 (33.85-35.64)	35.32 ± 0.86 (33.73-36.06)	34.87 ± 0.82 (33.23-36.06)
pH	7.83 ± 0.04 (7.76-7.90)	7.85 ± 0.08 (7.71-7.93)	7.90 ± 0.05 (7.84-8.00)	7.92 ± 0.08 (7.75-8.01)	7.88 ± 0.08 (7.71-8.01)
OSS (%)	86.01 ± 1.54 (82.65-87.99)	93.91 ± 4.12 (87.92-99.93)	74.24 ± 14.20 (37.13-100.44)	86.88 ± 4.98 (77.55-95.02)	85.26 ± 10.44 (37.13-100.44)

Table 4: Physical and chemical properties values collected during neap and spring tides under temporal sampling conditions.

(r=0.73, p<0.05) clearly shows that the pH values are not entirely ruled by estuary dynamics, where tidal currents dominate the coastal dynamics, carrying tropical water into the Caravelas estuary, but also by biogeochemical processes occurring within the MZ (see Discussion, Section Longitudinal sample).

The parameters of the carbonate system along neap and spring tides, during both the dry and rainy seasons can be found in Table 5.

Higher concentrations of the HCO^{3-} and TA variables involved in the carbonate system were observed in the dry season (Table 5). The dry season appears to potentiate the CO_2 from: The atmosphere or the respiratory activity of bacteria in order to decompose the organic matter produced by mangroves; and anthropic sources, which can also react with these shells, solubilizing biogenic calcium carbonate and generating an increase in TA and HCO^{-}_{3}. The average values of ρCO_2 shown in Table 5 between neap and spring cycles are similar in both studied seasons [55]. ρCO_2 seasonal averages (Table 5) hide the short-term temporal variation generated by tides (Figure 2). The largest ρCO_2 peaks are found during ebb tide. The processes which are responsible for such peaks are discussed in section longitudinal sample.

Oxygen saturation state is not particularly influenced by seawater (r < 0.50; p<0.05), which averages that they are independent processes, such as: the decomposition of organic matter, adsorption/desorption reactions, the nature of organic matter, and the re-suspension of bottom sediments (Table 4).

Balance of properties

Using Hansen and Rattray's stratification-circulation diagram (Section Analyses), our estuary was classified as Type 1a, which is weakly stratified during the neap tide and well-mixed during the spring tide. The Richardson number takes into account the fact that the river discharges water by diluting the seawater in the MZ. Thus, it can be thought of as a source of traction force and is associated with the horizontal stratification of density, which is in turn associated with the low frequency variation of the river discharge.

From measurements of: currents and hydrographic properties during neap-spring tides in the dry and rainy seasons, respectively, and estimated discharge values for the Caravelas River by Pereira et al. [56], which were 4-5 m/s during both campaigns, we calculated the numbers of the estuarine Richardson Ri_e as defined by eq. (2).

For each sample condition of the estuary, the Ri_e was determined as being equal to 3.52 and 0.29 in the conditions of the neap and spring tides in the dry season, respectively, and 0.003 and 0.15, respectively, in the rainy season. Therefore, according to the values found for Ri_e and within the criteria established by Fisher (1976), even though the studied estuary has its characteristics modified in dry and rainy periods, it may be classified as partially mixed in the first case and well mixed in the second. This concurs with the estuary classification according to the criterial of Hansen and Rattray, and the diagram obtained by Schettini and Miranda; Pereira et al. [39,55-57].

In general, for these types of estuary, the transport of salt up-estuary is due only to a turbulent diffusion process, while the residual flow is down-estuary at all depths.

In particular, the very small value Ri_e=0.003, which was found in our estuary in the neap tide condition in the rainy season campaign, is indicative of the fact that the residual flow can take place upwards in the estuary, in which the turbulent diffusion process is more efficient at transporting properties than the advective terms of river discharge and the Stokes transport taken together. This characterizes the estuary in this condition as an importer of properties. This importer feature, which was present at the neap tide of the rainy season, was also observed by Pereira et al., who analyzed the influences of salt transport mechanisms and suspended particulate matter (seston) on the Caravelas estuary under the same observation conditions as in this research. The work of these authors estimated balances among these various transport mechanisms and their influences on the transport of salt and suspended particulate matter (seston).

The values, which were calculated according to Bérgamo et al. [58], were 0.003 m/s and 0.04 m/s under the neap and spring tide conditions, respectively. However, in the rainy season, calculations of this same variable indicated that the residual movement at the neap tide, although virtually zero at -0.006 m/s, was up-estuary, while at spring tide, with a value of 0.02 m/s, it was down-estuary.

Tables 5 and 6 shows the values for the transport of the substances analyzed per width unit of the cross-section of the estuary. Since such substances were sampled in a single column of estuarine water during the four tide-cycles examined, negative values indicate an up-estuary direction, and positive values down-estuary.

According to the parameters of Table 6, it is expected that in the overall balance of transport of the substances analyzed in the present work, the estuary should present general conditions to export them. This export can be estimated by performing an annual review of the chemical properties listed in Table 6, and considered by way of an approximation that their respective fluxes happen uniformly through the straight section of the estuary. Performing this calculation, even if approximate, allows the results obtained in this work to be compared with measurements taken in other estuaries by other authors.

The annual reviews of the examined substances are shown in Table 7. The results show that the Caravelas estuary, in an annual cycle, acts as an exporter of all of the substances analyzed in this work, except from salinity.

This apparently contradictory scenario, which is due to the low

Properties	Dry season		Rainy season	
	Neap	Spring	Neap	Spring
TA (μmol kg^{-1})	2558 ± 40 (2469-2615)	2758 ± 140 (2549-2987)	2127 ± 134 (1912-2367)	2172 ± 70 (2070-2273)
$CO_{2\ (aqueous)}$ (μmol kg^{-1})	21.93 ± 2.69 (17.58-26.79)	21.86 ± 4.72 (15.49-30.66)	13.28 ± 2.02 (9.14-15.97)	13.26 ± 3.43 (9.98-20.49)
CO_3 (μmol kg^{-1})	196 ± 19 (164-236)	234 ± 50 (150-295)	220 ± 35 (184-306)	233 ± 43 (149-297)
HCO_3 (μmol kg^{-1})	2067 ± 57 (1958-2142)	2185 ± 101 (1931-2302)	1601 ± 111 (1368-1732)	1626 ± 88 (1513-1760)
DIC (μmol kg^{-1})	2285 ± 47 (2184-2350)	2441 ± 113 (2208-2609)	1834 ± 125 (1616-2028)	1872 ± 71 (1772-1976)
PCO_2 (μatm)	776 ± 91 (620-929)	775 ± 160 (559-1073)	508 ± 78 (349-612)	499 ± 132 (373-776)
pK*2 (mol kg^{-1})	9.43 ± 0.01 (9.42-9.45)	9.43 ± 0.01 (9.41-9.45)	9.38 ± 0.01 (9.36-9.40)	9.40 ± 0.02 (9.37-9.42)
Ω Calc	4.76 ± 0.43 (4.03-5.53)	5.52 ± 1.02 (3.80-6.83)	5.28 ± 0.77 (4.44-7.14)	5.46 ± 0.85 (3.73-6.80)
Ω Arag	3.13 ± 0.28 (2.65-3.65)	3.64 ± 0.68 (2.50-4.52)	3.52 ± 0.51 (2.96-4.76)	3.63 ± 0.63 (2.48-4.52)

Table 5: Chemical properties values collected during neap and spring tides under temporal sampling conditions.

Properties	Dry season		Rainy season		Mean
	Neap	Spring	Neap	Spring	
Salinity (kg/s/)	0.67	9.95	-1.55	4.43	3.38
TA (μmol/s)	48.34	780.01	-94.86	271.52	251.25
DIC (μmol/s)	42.60	680.01	-80.71	230.85	218.19
CO_3^{2-}(μmol/s)	3.65	67.03	-9.74	29.35	22.57
HCO^-_3 (μmol/s)	38.54	670.56	-70.40	199.91	209.65

Table 6: Seasonal transport parameters measured during four tide cycles under study conditions.

Properties	Caravelas estuary (This study)	Sepetiba bay (Ovalle et al.)
Salinity (Mg/year)	-1.76 × 10^5	9.28 × 10^{-4}
TA (kmol/year)	7.92	-
CO_3^{2-} (kmol/year)	0.71	-
HCO^-_3 (kmol/year)	6.11	- 0.02
DIC (kmol/year)	6.88	-

Table 7: Annual properties balance of this study and some literature data. Negative values mean importation of properties.

freshwater discharge of the estuary, could be explained by the additional supply of freshwater carried by the Peruípe River through a short width channel that is approximately 27 km long and connects that river to the estuary (Figure 1). This can be demonstrated by the values of the average profiles taken at the time of the u-velocity component around an observation point near the channel outlet in the estuary in the same tide conditions. Such results indicate residual movement through the channel from the Peruípe River to the estuary during all tide-cycles.

It is instructive to estimate the "effective" flux of the TA, HCO^-_3 and CO_3^{2-} of these variables for this particular estuary. The annual quantity of exported TA, HCO^-_3 and CO_3^{2-} is 7.92 kmol, 6.11 kmol and 0.71 kmol, respectively (Table 7). The total DIC flux (dissolved inorganic carbon) from the rivers to the ocean is 35 Tmol/year [59,60]. The export flux of the present study of the DIC is=6.88 kmol/year, and represents only 5 × 10^{-6} percent of the total world riverine DIC flux.

In reality, our DIC export data does not confirm that the estuary acts as a sequestration agent or a source of CO_2; on the contrary, the biogeochemical processes in the MZ or above may be sequestering or releasing CO_2 into the atmosphere. More conclusive studies involving this estuary and others on the Brazilian coast are important if we are to acquire a clear understanding of the role that estuaries play in CO_2 sequestration. If biogeochemical processes occurring within the MZ for each estuary ecosystem are considered in isolation, such an ecosystem does not become representative in relation to the particular area of the ocean. However, if the total area of this ecosystem (all of the estuaries on the planet combined) is considered, it becomes quite representative due to the highly reactive issues concerning the biogeochemical processes that occur [7].

Air-sea CO_2 fluxes

Recently, coastal areas have been attracting a great deal of attention due to CO_2 fluxes [61-65]. These researchers generated these CO_2 fluxes as they were motivated by attempts to understand: the effect CO_2 has on climate change and ocean acidification, and the role coastal areas play in CO_2 sequestration. Irrespective of their motivations, the values

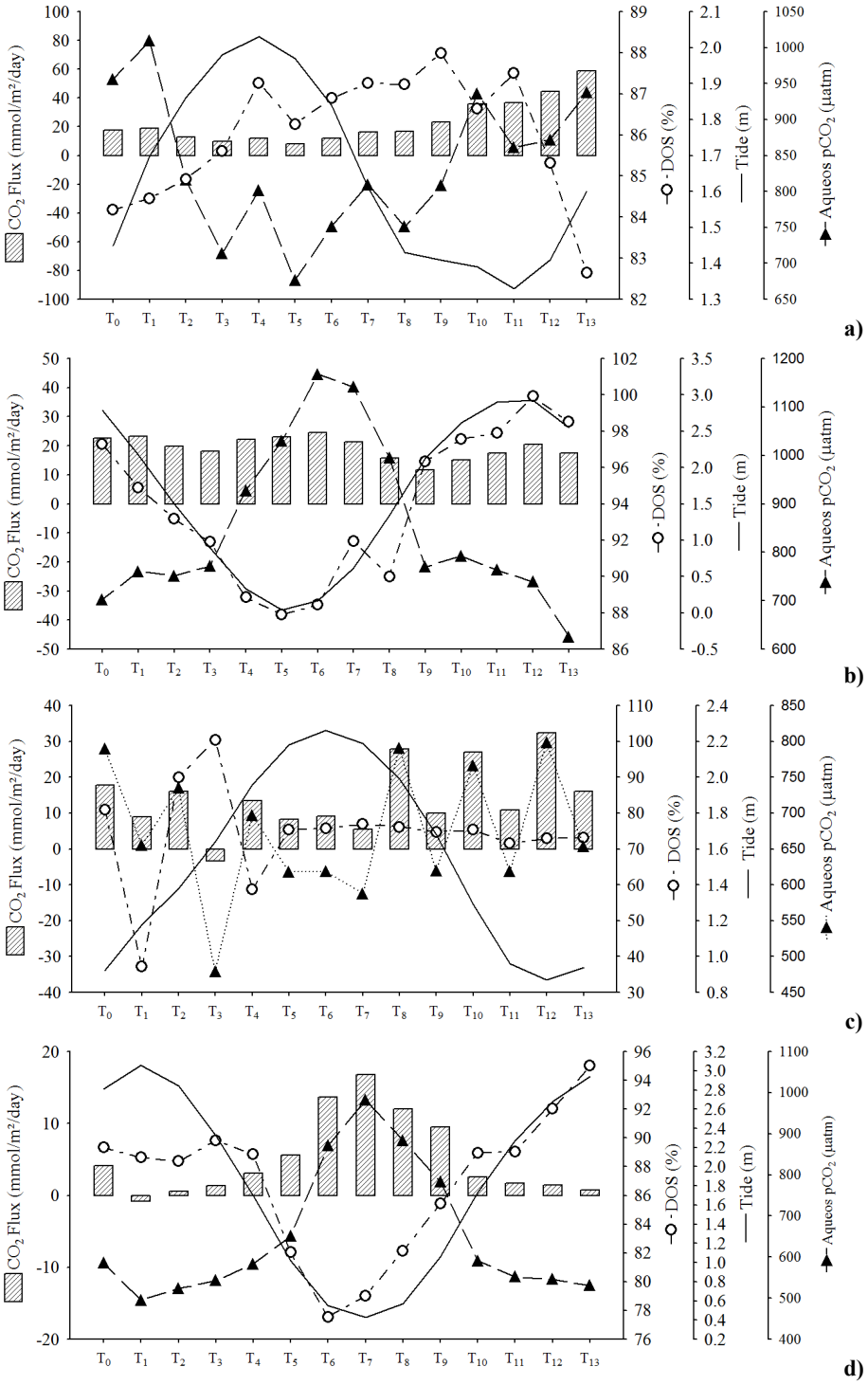

Figure 2: CO_2 temporal flux (13 h) from spot S1, Caravelas estuary. OSS: Oxygen saturation state: a) Neap tide cycle, dry season; b) Spring tide cycle, dry season; c) Neap tide cycle, rainy season; and d) Spring tide cycle, rainy season.

generated by these CO_2 fluxes are inaccurate in terms of the interface between water and air. Indeed, fundamental physical K, such as the Schmidt number and the gaseous exchange coefficient (kT) components of the flux equation, are limited when considered in field experiments once they are empirically generated in controlled laboratory conditions. Such K do not consider other factors that interfere with the CO_2 flux, such as: 1) The water/air turbulence interface, 2) Air bubbles, 3) Surfactant substances, 4) The water/air stability interface, and 5) Precipitation [46,65]. Accordingly, such factors, among others, are not linked with kT due to current knowledge limitations; wind

speed is the only variable that is used in the study of fluxes (Equation 4). Along with the previously mentioned physical factors, the K and thermodynamic components have an important influence on the CO_2 flux. This is because it is through these thermodynamic components $\left(\text{i.e., } k_0^*, k_1^*, k_2^*, HCO_3^-, CO_{2(aq)}, CO_{2(saturated)}\right)$ that the CO_2 flux is obtained via eq. (3), which also contains the physical K. Consequently, the CO_2 flux is obtained by way of physical and thermodynamic K.

As has been described above, the physical K used for the CO_2 flux estimation is limited. Conversely, the K and thermodynamic components are obtained from a number of carbonate system pairs such as pH and AT, and pH and DIC, the accuracy of which are determined in a laboratory [66]. Such parameters obtained in a laboratory provide software with information that generates accurate and transparent data about the carbonate system and the CO_2 fluxes. Results obtained this way can be compared with what the literature sustains such as by Millero et al. [3], Zeebe and Wolf-Gladrow [2], among others.

The CO_2 flux values in this article throughout the dry and rainy seasons, and during the neap and spring tides, remained within a positive variation range, which represents a supply of between 5 and 23 mmol/m^2/day of CO_2 to the atmosphere (Figure 2). On the whole, the highest average fluxes were observed during the neap and spring tide-cycles as well as during the ebb tide (respectively from 14 to 23 mmol/m^2/day and from 15 to 19 mmol/m^2/day). The highest flux values were measured during the ebb tide period, and might have been under the influence of waters originating from the estuary's upper MZ, the chemical composition of which is affected by a dense layer of mangroves and a small ratio between the small volume of the canal and a large area covered by mangroves (m^3/m^2). Such an occurrence results in organic carbon being supplied to the estuarine channel. This originated from the mangrove (mangrove debris, microphytobenthos and dissolved organic compounds) or allochthonous (non-mangrove) forests, which are decomposed by the respiratory activity of bacteria. This water is transported during the ebb tide and has the highest aqueous ρCO_2 records, which are clearly evident during spring tide-cycles in both the rainy and dry seasons (respectively, 1,073 and 776 µatm; Figure 2). During the spring tide-cycles, an increase in aqueous ρCO_2 was well evidenced due to respiratory activity, where the lowest values of dissolved oxygen saturation during both the dry and rainy seasons were 87.92% and 77.55%, respectively (Figure 2).

The Caravelas estuary sent CO_2 off into the atmosphere along monitored cycles, which characterize the system as heterotrophic [60]. The annual flux recorded in this work was estimated to be 6 mol/m^2/year, which is close to the value approximated for the open ocean (<3 mol/m^2/year) [67]. On the other hand, the values obtained in this work were considerably lower than those estimated for estuarine systems by Koné and Borges [68], Paz et al. [69], Cai and Wang [8] and Abril et al. [70], which were, respectively: 37 mol/m^2/year, 4037 mol/m^2/year, 15 mol/m^2/year and 4–241 mol/m^2/year. Abril and Borges [70] discussed flux values found by researchers using different sampling techniques. However, the techniques used are not discussed as far as the thermodynamic approach is concerned.

Finally, such an estuarine system is an exporter of inorganic carbon to the adjacent coastal marine system as DIC, and into the atmosphere as CO_2.

Conclusion

A very wide range of results has been produced with respect to the CO_2 flux in coastal marine environments. The biological metabolism of the marine system is partly responsible for this, but the sampling design and analytical procedures used may have also made, in the case of estuaries, a major contribution to this. Consequently, there is still a great deal of uncertainty as far as gaseous CO_2 fluxes in such systems are concerned. Moreover, the simple extrapolation of results found in estuarine systems to a global scale still needs to be rethought. Accordingly, the thermodynamic approach within an international protocol for studies of fluxes in estuarine systems should be defined as the standard measure. We suggest that further research should be carried out to provide a larger, more spatially and temporally resolved estimates of water-to-air transfer of CO_2 to refine our estimates of CO_2 in estuaries, considering the drainage system of mangrove forests and their role as a source of CO_2 to the atmosphere.

Acknowledgements

The authors are grateful to all students involved in the field activities and, especially to Dr. Carlos A. F. Schettiniand and Dr. Marçal D. Pereira for CTD and ADCP data. Martins, G. for English review. We would like to thank IEAPM, especially the technical support provided by Natália P. Saraiva da Silva and Gilberto de J. de Oliveira. The Pro-Abrolhos Project is mainly supported by the Brazilian National Research Council–CNPq, through the Instituto do Milênio Program (Projeto PRO-ABROLHOS 420219/2005-6).

References

1. Abril G, Frankignoulle M (2001) Nitrogen-alkalinity interactions in the highly polluted Scheldt basin (Belgium). Water Res 35: 844-850.
2. Zeebe RE, Wolf-Gladrow D (2001) CO_2 in Seawater: equilibrium, kinetics, isotopes. Elsevier Oceanography Series 65: 1-341.
3. Millero FJ (2006) Chemical Oceanography, third Ed. CRC Press, Boca Raton.
4. RamoseSilva CA (2011) Oceanografia Química. Rio de Janeiro: Ed. Interciência.
5. Frankignoulle M, Abril G, Borges A, Bourge I, Canon C (1998) Carbon dioxide emission from European estuaries. Science 282: 434-436.
6. RamoseSilva CA, Silva AP, Oliveira SR (2006) Concentration, stock and transport rate of heavy metals in a tropical red mangrove, Natal-Brazil. Mar Chem 99: 2-11.
7. Ramos e Silva CA, Oliveira SR, Rêgo RDP, Mozeto AA (2007) Dynamics of phosphorus and nitrogen through litter fall and decomposition in a tropical mangrove forest. Mar Environ Res 64: 524-534.
8. Cai WJ, Wang Y (1998) The chemistry, fluxes, and sources of carbon dioxide in the estuarine waters of the Satilla and Altamaha, Rivers, Georgia. Limnol Oceanogr 43: 657-668.
9. RamoseSilva CA, Miranda LB, Dávalos PB, Silva MP (2010) Hydrochemistry in tropical hyper-saline and positive estuaries. Pan-Am J Aqua Sci 5: 432-443.
10. Ruiz-Halpern S, Maher DT, Santos IR, Eyre BD (2014) High CO_2 evasion during floods in an Australian subtropical estuary downstream from a modified acidic floodplain wetland. Limnol Oceanogr 60: 42-56.
11. Marotta H, Duarte CM, Pinho L, Enrich-Prast A (2010) Rainfall leads to increased ρCO_2 in Brazilian coastal lakes. Biogeosciences 7: 1607-1614.
12. Millero FJ (1986) The pH of estuarine waters. Limnol Oceanogr 31: 839-847.
13. Dickson AG, Sabine CL, Christian JR (2007) Guide to best practices for ocean CO_2 measurements. PICES Special Publication 3: 1-191.
14. Wolf-Gladrow DA, Zeebe RE, Klaas C, Körtzinger A, Dickson AG (2007) Total alkalinity: The explicit conservative expression and its application to biogeochemical processes. Mar Chem 106: 287-300.
15. Feely RA, Sabine CL, Lee K, Berelson W, Kleypas J, et al. (2004) Impact of anthropogenic CO_2 on the $CaCO_3$ system in the oceans. Science 305: 362-366.
16. Milligan AJ, Mioni CE, Morel FMM (2009) Response of cell surface pH to pCO_2 and iron limitation in the marine diatom Thalassiosiraweissflogii. Mar Chem 114: 31-36.
17. Wilson RW, Millero FJ, Taylor JR, Walsh PJ, Christensen V, et al. (2009) Contribution of fish to the marine inorganic carbon cycle. Science 323: 359-362.

18. Krauskopf KB, Bird DK (1995) Introduction to geochemistry. New York. McGraw-Hill.
19. Gattuso JP, Lavigne H (2009) Technical Note: Approaches and software tools to investigate the impact of ocean acidification. Biogeosciences 6: 2121-2133.
20. Gattuso JP, Frankignoul M, Smith, SV (1999) Measurement of community metabolism and significance in the coral reef CO_2 source-sink debate. P Natl Acad Sci U S A 96: 13017-13022.
21. Knoppers BA, Ekau W, Figueredo AG (1999) The coast and shelf of east northeast Brazil and material transport. Geo-Mar Lett 19: 171-178.
22. Defant A (1960) Physical Oceanography. Oxford: Pergamon Press 2: 598.
23. Franco AS (2000) "MARÉS: Programa para Previsão e Análise". In: Manual, BSP São Paulo p: 36.
24. Grasshoff K, Ehrhardt M, Kremling K (1983) Methods of seawater analysis. Verlang Chemie, Nurnberg.
25. DOE (1994) Handbook of methods for the analysis of the various parameters of the carbon dioxide system in sea water. Version 2. In: Dickson AG, Goyet C. (Eds.) ORNL/CDIAC 74.
26. VandenBerg CMG, Rogers H (1987) Determination of alkalinities of estuarine waters by a two-point potentiometric titration. Mar Chem 20: 219-226.
27. Millero FJ, Zhang JZ, Fiol S, Sotolongo S, Roy RN, et al. (1993) The use of buffers to measure the pH of seawater. Mar Chem 44: 143-152.
28. Clayton TD, Byrne RH (1993) Spectrophotometric seawater pH measurements: total hydrogen ion concentration scale calibration of m-cresol purple and at-sea results. Mar Chem 40: 2115-2129.
29. Nemzer BV, Dickson AG (2005) The stability and reproducibility of Tris buffers in synthetic seawater. Mar Chem 96: 237-242.
30. Pérez FF, Fraga F (1987) The pH Measurements in seawater on the NBS Scale. Mar Chem 21: 315-327.
31. Millero FJ (1996) Chemical Oceanographic. In: Michael J, Kennishi and Lutz PL (eds.), Florida/USA.
32. Millero FJ (2000) Phisycal chemistry of natural waters. Wiley-interscience.
33. Dickson AG (1990) Standard potential of the AgCl(s)+½ H2(g)=Ag(s)+HCl(aq) cell and the dissociation constant of bisulfate ion in synthetic sea water from 273.15 to 318.15 K. J Chem Thermodyn 22: 113-127.
34. Yao W, Millero FJ (1994) The chemistry of the anoxic waters in the Framvaren Fjord, Norway. Aquat Geochem 1: 53-88.
35. Roy RN, Roy LN, Vogel KM, Porter-Moore C, Pearson T, et al. (1993) Determination of the ionization constants of carbonic acid in seawater. Mar Chem 44: 249-268.
36. Sabine CL, Feely RA, Gruber N, Key RM, Lee K, et al. (2004) The oceanic sink for anthropogenic CO_2. Science 305: 367-371.
37. Pankow JF (1991) Aquatic Chemistry Concepts. CRC Press, Boca Raton.
38. Miranda LB, Castro BM, Kjerfve B (2002) Princípios de oceanografia física de estuários. EDUSP, São Paulo.
39. Hansen DV, Rattray M (1966) New dimensions in estuary classification. Limnol Oceanogr 11: 319-326.
40. Fischer HB, (1976) Mixing and dispersion in estuaries. Annu Rev Fluid Mech 8: 107-133.
41. Bowden KF (1963) The mixing processes in a tidal estuary. Inter J Air Water Pollut 4: 343-356.
42. Bowden KF (1978) Mixing processes in estuaries. In: Kjerfve, Belle B, Baruch W (eds.) Estuarine transport processes, Library In Marine Science, No. 7, University of South Carolina Press, Columbia, S.C., pp: 11-36.
43. Dyer KR, New AL (1986) Intermittency in estuarine mixing. In: Wolfe DA (ed.) Estuarine variability. Orlando, Fla.: Academic Press pp: 321-339.
44. Jähne B, Heinz G, Dietrich W (1987) Measurement of the diffusion coefficients of sparingly soluble gases in water. J Geophys Res 92: 10767-10776.
45. Jähne B, Munnich KO, Bosinger R, Dutzi A, Huber W, et al. (1987) On the parameters influencing air-water gas exchange. J Geophys Res 92: 1937-1949.
46. Wanninkhof R (1992) Relationship between wind speed and gas exchange over the ocean. J Geophys Res 97: 7373-7382.
47. Smith EM, Kemp WM (2001) Size structure and the production/respiration balance in a coastal plankton community. Limnol Oceanogr 46: 473-485.
48. Miranda LB, Castro BM, Kjerfve B (2008) In Princípios de Oceanografia Física de Estuários. São Paulo: Editora da Universidade de São Paulo p: 419.
49. RamoseSilva CA (2004) Análise físico-químicas de sistemas marginais marinhos. Interciência, Rio de Janeiro.
50. Millero FJ (1997) Laboratory for chemical oceanography. Rosenstiel School of Marine Atmospheric Science. University of Miami, FL, USA.
51. Chester R (1990) Marine Biochemistry. Unwin Hyman, London.
52. Cai WJ (2011) Estuarine and coastal ocean carbon paradox: CO_2 sinks or sites of terrestrial carbon incineration? Ann Rev Mar Sci 3: 123-145.
53. Tynan E, Clarke JS, Humphreys MP, Ribas-Ribas M, Esposito M (2016) Physical and biogeochemical controls on the variability in surface pH and calcium carbonate saturation states in the Atlantic sectors of the Arctic and Southern Oceans. Deep Sea II 127: 7-27.
54. Bayraktarov E, Price RE, Ferdelman TG, Finster K (2013) The pH and pCO_2 dependence of sulfate reduction in shallow submarine hydrothermal CO_2-venting sediments (Milos Island, Greece). Frontiers in Microbiology 4: 111.
55. www.inmet.gov.br/portal/index.php?r=home/page&page=rede_estacoes_auto_graf
56. Pereira MD, Siegle E, Miranda LB, Schettini CAF (2010) Hydrodynamics and transport of particulate matter in seasonal suspension in a tidal dominated estuary: Caravelas estuary (BA). Revista Brasileira de Geofísica 28: 427-444.
57. Schetinni CAF, Miranda LB (2010) Circulation and suspended particulate matter transport in a tidally dominated estuary: Caravelas estuary, Bahia, Brazil. Braz. J Oceanogra 58: 1-11.
58. Bérgamo AL, Miranda LB, Corrêa MA (2002) Estuary: Programs for processing and analysis of hydrographic and correntographic data.Relatório Técnico. Instituto Oceanográfico, São Paulo 49: 1-16.
59. Garrels RM, Mackenzie, FT (1972) A quantitative model for the sedimentary rock cycle. Mar Chem 1: 27-41.
60. Kempe S, Cauwet G (1991) Biogeochemistry of Europe rivers. In: Degens ET, Kempe S, Richey JE (eds.) Biogeochemistry of major world rivers. SCOPE 42. John Wiley & Sons.
61. Troxlera TG, Barrb JG, Fuentesc JD, Engeld V, Andersond G (2015) Component-specific dynamics of riverine mangrove CO_2 efflux in the Florida coastal Everglades. Agr Forest Meteorol (in press).
62. Bates NR (2012) Seasonal variability of the effect of coral reefs on seawater CO_2 and air-sea CO_2 exchange. Limnol Oceanogr 47: 43-52.
63. Zhaia W, Dai M (2009) On the seasonal variation of air-sea CO_2 fluxes in the outer Changjiang (Yangtze River) Estuary, East China Sea. Mar Chem 117: 2-10.
64. Zhaia W, Daia M, Caic WJ, Wangc Y, Honga H (2005) The partial pressure of carbon dioxide and air-sea fluxes in the northern South China Sea in spring, summer and autumn. Mar Chem 96: 87-97.
65. Borges AV, Vanderborght JP, Schiettecatte LS, Gazeau F, Ferron-Smith S, at al. (2004) Variability of the gas transfer velocity of CO_2 in a macrotidal estuary (the Scheldt). Estuaries 27: 593-603.
66. Dickson AG (2010) The carbon dioxide system in seawater: equilibrium chemistry and measurements. Guide to best practices for ocean acidification research and data reporting.
67. Smethie WM, Takahashi T, Chipman DW, Ledwell JR (1985) Gas exchange and CO_2 flux in the tropical Atlantic ocean determined from 222Rn and p CO_2 measurements. J Geophys Res 90: 7005-7022.
68. Koné YJM, Borges AV (2008) Dissolved inorganic carbon dynamics in the waters surrounding forested mangroves of the Ca Mau Province (Vietnam). Estuar Coast Shelf S 77: 409-421.
69. Paz M, Padín XA, Ríos AF, Pérez FF (2010) Surface fCO_2 variability in the Loire plume and adjacent shelf Waters: High spatio-temporal resolution using ships of opportunity. Mar Chem 118: 108-118.
70. Abril G, Borges AV (2004) Carbon dioxide and methane emissions from estuaries, in: Greenhouse Gas Emissions: Fluxes and Processes. Hydroelectric Reservoirs and Natural Environments. Environmental Science Series, Springer-Verlag.